Quantum reading capacity under thermal and correlated noise

Quantum reading capacity under thermal and correlated noise

Cosmo Lupo,[1,2] Stefano Pirandola,[3] Vittorio Giovannetti,[4] and Stefano Mancini[2,5]
[1]*MIT, Research Laboratory of Electronics, 77 Massachusetts Avenue, Cambridge MA 02139, USA*
[2]*School of Science and Technology, University of Camerino, Via Madonna delle Carceri 9, I-62032 Camerino, Italy*
[3]*Department of Computer Science, University of York, Deramore Lane, York YO10 5GH, United Kingdom*
[4]*NEST, Scuola Normale Superiore and Istituto Nanoscienze-CNR, Piazza dei Cavalieri 7, I-56126 Pisa, Italy*
[5]*INFN-Sezione di Perugia, Via A. Pascoli, I-06123 Perugia, Italy*
(Received 11 December 2012; published 10 June 2013)

Quantum communication theory sets the maximum rates at which information can be encoded and decoded reliably given the physical properties of the information carriers. Here we consider the problem of readout of a digital optical memory, where information is stored by means of the optical properties of the memory cells that are in turn probed by shining a laser beam on them. Interesting features arise in the regime in which the probing light has to be treated quantum mechanically. The maximum rate of reliable readout defines the *quantum reading capacity*, which is proven to overcome the classical reading capacity—obtained by probing with classical light—in several relevant settings. We consider a model of optical memory in which information is encoded in the (complex-valued) attenuation factor and study the effects on the reading rates of thermal and correlated noise. The latter type of noise arises when the effects of wave diffraction on the probing light beam are taken into account. We discuss the advantages of quantum reading over the classical one and show that the former is substantially more robust than the latter under thermal noise in the regime of low power per pulse.

DOI: 10.1103/PhysRevA.87.062310 PACS number(s): 03.67.Hk, 42.30.−d, 42.50.Ex

I. INTRODUCTION

Data storage devices make use of different stable or metastable states of suitable physical systems, typically organized in arrays of memory cells, which are employed to store classical information. In turn, the process of retrieving the stored information involves a second physical system used to probe the state of the cells. The readout process is hence made of three steps: (1) the probing system is prepared in a given initial state; (2) the memory cells and the probe interact according to the their physical properties; (3) the probe is collected and measured in order to extract the information encoded in the state of memory cells mirrored in the final state of the probing system. The prototypical example is that of digital optical memories, such as CDs, DVDs, and BDs, where information is stored in digital form according to the optical properties of the memory cells. In this case, the readout process consists of shining a laser on the memory cells, whose reflected beam is then collected and properly measured. Under standard conditions, the use of classical coherent light with a macroscopic number of photons is sufficient to guarantee a faithful readout process with negligible probability of error. On the other hand, this is no longer true in the regime of weak signals in which quantum fluctuations become predominant and, due to the uncertainty principle, forbid the faithful discrimination of coherent states. Remarkably, as it was first pointed out in [1], it is in the few photon regime that *nonclassical* states of light can provide the optimal probing states for the readout of a classical memory, hence overcoming the performances of classical light sources. This result, which is already interesting by its own, may open the way to novel applications of quantum optics for data storage technologies, e.g., by increasing the data storage capacity or the readout rate or by allowing the safe and faithful readout of photodegradable memories.

A model for studying the readout of digital classical memories in the quantum regime was first considered in [1]. There, a model of memory was introduced in which information is encoded in a binary fashion according to the optical reflectivity of each memory cell. That is, a low or high reflectivity of the memory cell is used to store one bit of classical information. Hence, depending on the reflectivity value, a beam of light impinging on a memory cell results in an attenuated amplitude of the reflected beam. It follows that the problem of the memory readout is naturally formulated as the problem of *statistical discrimination* between two *lossy bosonic channels* [1,2], and its probability of success arises as a suitable performance quantifier. Variants of this model include the cases in which the interaction with the memory cell affects other optical properties of the reflected beam, as phase [3] or both phase and amplitude [4]. Other variants consider the case where both the ports of the *beam-splitter* memory cell are available to the probing light, with the problem of readout becoming equivalent to a discrimination of unitaries [5,6]; see also [7,8].

Moving beyond the case of the readout of a single bit of information encoded in a memory cell, one has to consider the more realistic setting for data storage devices in which information is encoded in (long) arrays of memory cells. Classical error correcting codes are also used to further reduce the probability of faulty readout. General coding theorems (see, e.g., [9]) can be applied to this setting to provide expressions for the maximum rates at which information can be *reliably* retrieved in the reading process. In particular, when the memory cells are probed by a quantum system, the asymptotically optimal and reliable readout rate is given in terms of the *Holevo information* [10]. In this context one can distinguish two main settings defined by the physical properties of the probing states. In the first one the quantum probe is initialized in a "classical" state, that is, a state characterized by

a positive Sudarshan-Glauber quasidistribution [11]. Classical states can be written as convex combinations of coherent states and have a well-defined classical limit for $\hbar \to 0$. On the other hand, nonclassical states are those that show typical quantum features, for instance squeezing, entanglement, and nonlocality. In both cases, we allow the presence of an ancillary system in order to exploit (classical or quantum) correlations with the probe. The *classical reading capacity* is hence defined as the maximum rate of reliable memory readout achievable when the state of the probe and ancillary systems is a classical one. More generally, the *quantum reading capacity* is the maximum rate over arbitrary quantum states, including nonclassical ones [12]. An explicit expression for the classical reading capacity was computed in [12], as a function of the mean photon number of the probing light. While the calculation of the quantum reading capacity remains an open problem, several examples were provided of nonclassical states outperforming all the classical ones [12], hence proving that the quantum reading capacity is strictly greater than its classical counterpart in several settings.

Here we examine the quantum reading capacity of a classical digital memory in the presence of different kinds of noise. For given mean photon number impinging on each memory cell, we compare the classical reading capacity with that achievable by an entangled state of the probe and ancillary systems, which possess Einstein-Podolsky-Rosen (EPR) correlations. First, we provide analytical expressions in the presence of thermal background in the limit of faint signals, showing that the reading rate with the entangled EPR state probing is unaffected by thermal-like noise. Second, we provide bounds on the quantum reading rates in the presence of correlated noise due to light diffraction [13]. Indeed, wave diffraction of the reflected light causes cross talks among signals scattered by neighboring memory cells. Notwithstanding a potential reduction of the reading rates, we show that the separation between classical and quantum probing persists in the presence of this kind of correlated noise.

The article proceeds as follows. In Sec. II we review the quantum reading in the optical framework and in Sec. III we analyze the case of quantum reading in the presence of background thermal noise. In Sec. IV we introduce and characterize the effects of diffraction in quantum reading. Finally, Sec. V contains conclusions and remarks. Appendix contains detailed calculations regarding the quantum description of diffraction.

II. QUANTUM READING CAPACITY OF OPTICAL MEMORIES

We consider a model of classical optical memory consisting of a *long* array of $K \gg 1$ memory cells, where the jth cell encodes the d-ary variable $u(j)$ according to its optical reflectivity. Hence, a probing beam of light impinging on the jth cell will be attenuated by a complex-valued factor $z_{u(j)}$, describing both attenuation and delay. In order to optimize the memory performance we allow information to be encoded by means of a set of 2^C distinct code words $\mathbf{u}^i = [u^i(1),u^i(2),\ldots,u^i(K)]$ of length K, with $i = 1,\ldots,2^C$, at a rate of C/K bits per cell. These code words define a classical error correcting code for the memory. A quantum description of the interaction between the jth memory cell and the probing light is provided by an associated quantum channel $\phi_{u(j)}$ which maps the incoming beam of light into an attenuated one and accounts for the presence of background (thermal) noise. A single mode of incoming light, described by the canonical ladder operators a, $a^\dagger$, is hence transformed into an outgoing one according to the Heisenberg-picture transformation,

$$a \to z_{u(j)}\, a + \sqrt{1 - |z_{u(j)}|^2}\, v + \nu\,, \tag{1}$$

where v denotes an environmental "vacuum" mode, and ν is a Gaussian distributed classical random variable, with zero mean and variance $n_{\rm th}$, modeling the background thermal noise (note that an alternative way to introduce thermal noise is to consider an environmental thermal mode instead of a vacuum mode [1]). Associated with each code word of the error correction code there is a sequence of single-mode quantum channels $\phi_{u^i(1)} \otimes \phi_{u^i(2)} \otimes \cdots \phi_{u^i(K)}$. We define the marginal ensemble of quantum channels $\Phi = \{p_u,\phi_u\}$, where p_u is the relative fraction of instances of the channel ϕ_u among the code words. The ensemble Φ is also called the marginal cell of the memory [12].

Given the memory model, a reading protocol is characterized by the physical properties of the probing light. Here we consider a setting in which each memory cell is independently probed by a collection of s bosonic modes [14], described by the ladder operators $\{a_k,a_k^\dagger\}_{k=1,\ldots,s}$, which are jointly measured with r ancillary modes, which are in turn associated with the operators $\{b_{k'},b_{k'}^\dagger\}_{k'=1,\ldots,r}$. We refer to the collective state of the $s+r$ modes as the *transmitter*, and denote it as $\rho(s,r)$. The state of the transmitter after the interaction with a subarray of cells encoding the code word $\mathbf{u}^i$ reads

$$\rho_{\mathbf{u}^i}(s,r) = \bigotimes_{j=1}^{K} \rho_{u^i(j)}(s,r) = \bigotimes_{j=1}^{K} \left(\phi_{u^i(j)}^{\otimes s} \otimes I^{\otimes r}\right)[\rho(s,r)], \tag{2}$$

where I is the identity transformation acting on each of the ancillary modes. Finally, the last step of the reading protocol consists of performing a collective measurement on the outgoing light in order to discriminate among different code words. The discrimination can be performed flawless in the limit $K \to \infty$ by choosing optimal code words and collective measurements up to a rate given by the Holevo information [10]:

$$\chi[\Phi|\rho(s,r)] = S\left[\sum_u p_u \rho_u(s,r)\right] - \sum_u p_u S[\rho_u(s,r)], \tag{3}$$

where $S(\cdot) = -\mathrm{Tr}[(\cdot)\log_2(\cdot)]$ denotes the von Neumann entropy and $\rho_u(s,r) = (\phi_u^{\otimes s} \otimes I^{\otimes r})[\rho(s,r)]$.

The quantum reading capacity of a classical memory with marginal cell Φ is finally defined by optimizing the reading rate $\chi[\Phi|\rho(s,r)]$ over the choice of the probing state $\rho(s,r)$ [12]:

$$C(\Phi) = \sup_{s,r} \sup_{\rho(s,r)} \chi[\Phi|\rho(s,r)]. \tag{4}$$

However, one has to notice that $\chi[\Phi|\rho(s,r)]$ is upper bounded by the Shannon entropy of the ensemble Φ, $H(\Phi) = -\sum_u p_u \log_2 p_u$, which in turn can be made equal to $\log_2 d$ by letting p_u to be the flat distribution. It is easy to show that this bound is saturated by choosing $\rho(s,r)$ to be a pure state

and allowing s to be arbitrarily large [12]. For this reason, the quantum reading capacity is a nontrivial notion only when we optimize the transmitter state under a suitable constraint. In the framework of optical readout, the most meaningful physical constraint is given by fixing the mean number of photons impinging on each memory cell. Thus, we consider fixed-energy transmitters $\rho(s,r,n)$ defined as those transmitters $\rho(s,r)$ which irradiate an average of n photons on each memory cell, i.e., such that

$$\mathrm{Tr}\left[\rho(s,r,n)\sum_{k=1}^{s}a_k^\dagger a_k\right]=n\,. \tag{5}$$

We hence define the *constrained quantum reading capacity* by optimizing the reading rate over all the transmitters at fixed energy [12],

$$C(\Phi|n)=\sup_{s,r}\sup_{\rho(s,r,n)}\chi[\Phi|\rho(s,r,n)]. \tag{6}$$

Note that an alternative (local) energy constraint consists of fixing the mean number of photons per signal mode, as recently adopted in Refs. [15,16] — see [2] for more details on global and local energy constraints in quantum channel discrimination. Also note that a different definition of optical reading capacity has been recently given in Ref. [17], where an optimization on the marginal cell is implicitly considered.

In the following we evaluate bounds on $C(\Phi|n)$ by computing $\chi[\Phi|\rho(s,r,n)]$ for different choices of the transmitter. First, we consider the case of "classical" states—those having a positive Sudarshan-Glauber quasidistribution [11]—of $s+r$ modes. By restricting to classical transmitters, denoted as $\rho_{\mathrm{c}}(s,r,n)$, one defines the constrained *classical reading capacity*:

$$C_{\mathrm{c}}(\Phi|n)=\sup_{s,r}\sup_{\rho_c(s,r,n)}\chi[\Phi|\rho_c(s,r,n)]. \tag{7}$$

Classical states form a convex set whose extremal points are coherent states of $s+r$ modes. It was proven in [12] that for the noiseless case ($n_{\mathrm{th}}=0$) the optimal classical probing state is a single-mode coherent state with $s=1$ and $r=0$. Here we conjecture, supported by numerical evidence, that the same holds true even in the noisy case ($n_{\mathrm{th}}>0$). Second, we evaluate $\chi[\Phi|\rho(s,r,n)]$ for an exemplary "nonclassical" transmitter given by

$$\rho_{\mathrm{EPR}}(s,s,n)=(|\xi\rangle\langle\xi|)^{\otimes s}, \tag{8}$$

where

$$|\xi\rangle=(\cosh\xi)^{-1}\sum_{m=0}^{\infty}(\tanh\xi)^m|m\rangle_{S_k}|m\rangle_{R_k}, \tag{9}$$

with $\xi=\mathrm{arc\,sinh}\sqrt{(n/s)}$ and $|m\rangle_{S_k}=(m!)^{-1/2}(a_k^\dagger)^m|0\rangle$, $|m\rangle_{R_k}=(m!)^{-1/2}(b_k^\dagger)^m|0\rangle$ ($|0\rangle$ denoting the vacuum state). The transmitter $\rho_{\mathrm{EPR}}(s,s,n)$ is the tensor product of s EPR states, providing the simplest description of the output of parametric down conversion; see, e.g., [18], as well as the prototypical example of entangled state in the continuous-variable setting [2,19].

III. QUANTUM READING CAPACITY UNDER THERMAL NOISE

We start by considering the case of coherent state transmitters and introduce the quantity,

$$C_{\mathrm{coh}}(\Phi|n)=\sup_{s,r}\sup_{\rho_{\mathrm{coh}}(s,r,n)}\chi[\Phi|\rho_{\mathrm{coh}}(s,r,n)], \tag{10}$$

where

$$\rho_{\mathrm{coh}}(s,r,n)=\bigotimes_{k=1}^{s}|\alpha_k\rangle\langle\alpha_k|\bigotimes_{k'=1}^{r}|\beta_{k'}\rangle\langle\beta_{k'}|, \tag{11}$$

is a coherent state of $s+r$ modes and the photon-number constraint reads $\sum_{k=1}^{s}|\alpha_k|^2=n$.

First of all, we notice that since the state $\rho_{\mathrm{coh}}(s,r,n)$ is in the form of a direct product between the state of the probe and the state of the ancillary system, the subadditivity of the Holevo information implies that the presence of the ancillary modes cannot increase the reading rate, that is,

$$C_{\mathrm{coh}}(\Phi|n)=\sup_{s}\sup_{\rho_{\mathrm{coh}}(s,0,n)}\chi[\Phi|\rho_{\mathrm{coh}}(s,0,n)]. \tag{12}$$

We can hence restrict our attention to transmitters of the form $\rho_{\mathrm{coh}}(s,0,n)$ which, according to Eq. (1), are mapped into

$$\rho_{\mathrm{coh},u}(s,0,n)=\bigotimes_{k=1}^{s}\sigma_u(\alpha_k), \tag{13}$$

with

$$\sigma_u(\alpha_k)=\int d\nu_k G_{n_{\mathrm{th}}}(\nu_k)|z_u\alpha_k+\nu_k\rangle\langle z_u\alpha_k+\nu_k|, \tag{14}$$

where $G_{n_{\mathrm{th}}}(\nu_k)$ denotes a Gaussian probability density distribution with zero mean and variance n_{th}. Then, we notice that it is always possible to find a u-independent unitary matrix U such that, given the energy constraint, the coherent-state amplitudes in Eq. (14) transform as follows:

$$\sum_{k=1}^{s}U_{ik}(z_u\alpha_k+\nu_k)=\delta_{1i}z_u\sqrt{n}+\nu_i', \tag{15}$$

where the random variables ν_i''s are independent and identically distributed according to a Gaussian distribution with zero mean and variance n_{th}. The unitary transformation U on the coherent-state amplitudes can be physically implemented by a network of passive linear-optical elements, as beam splitters and phase shifter. Due to the unitary invariance of the von Neumann entropy such a transformation cannot change the value of the Holevo information, hence the final state of the transmitter can be assumed, without loss of generality, to be of the form,

$$\rho_{\mathrm{coh},u}(s,0,n)=\sigma_u(\sqrt{n})\otimes\sigma(0)^{\otimes(s-1)}, \tag{16}$$

where $\sigma(0)=\int d\nu G_{n_{\mathrm{th}}}(\nu)|\nu\rangle\langle\nu|$ is a u-independent thermal state. We notice that such a state is the tensor product of a state of the first probing mode and a u-independent state of the remaining $(s-1)$ modes. Once again, the subadditivity Holevo information implies that the presence of the $(s-1)$ probing modes cannot increase the Holevo function. In conclusion, we have obtained that a single-mode coherent state

is optimal among coherent state transmitters, that is,

$$C_{\rm coh}(\Phi|n) = \chi[\Phi|\rho_{\rm coh}(1,0,n)], \tag{17}$$

where we can assume without loss of generality $\rho_{\rm coh}(1,0,n) = |\sqrt{n}\rangle\langle\sqrt{n}|$.

We now consider the case of generic classical transmitters. First of all, since coherent states are classical states,

$$C_{\rm c}(\Phi|n) \geqslant C_{\rm coh}(\Phi|n). \tag{18}$$

On the other hand, any classical state $\rho_c(s,r,n)$ can be written as the convex sum of coherent states,

$$\rho_{\rm c}(s,r,n)=\int dy p_y \bigotimes_{k=1}^{s} |\alpha_k(y)\rangle\langle\alpha_k(y)| \bigotimes_{k'=1}^{r} |\beta_{k'}(y)\rangle\langle\beta_{k'}(y)|, \tag{19}$$

with $p_y \geqslant 0$ and $\int dy p_y = 1$. Using the convexity of the Holevo information we get

$$C_{\rm c}(\Phi|n) \leqslant \int dy p_y C_{\rm coh}(\Phi|n_y), \tag{20}$$

where $n_y = \sum_{k=1}^{s} |\alpha_k(y)|^2$ with $n = \int dy p_y n_y$. It is worth noticing that Eq. (20) does not suffice to conclude that $C_{\rm c}(\Phi|n) \leqslant C_{\rm coh}(\Phi|n)$. As already discussed in [12], a sufficient condition for having $C_c(\Phi|n) \leqslant C_{\rm coh}(\Phi|n)$ is that $C_{\rm coh}(\Phi|n)$ is in turn a concave function of n.

In the remainder of this section, we focus on the case of binary encoding where the marginal cell $\Phi \equiv \{p_0, p_1, z_0, z_1\}$ is identified by the probability weights p_0, $p_1 = 1 - p_0$, and by the complex valued attenuation factors z_0, z_1. In the noiseless case, $n_{\rm th} = 0$, an analytical expression for $C_{\rm coh}(\Phi|n)$ has been computed in [12] for (real) positive values of z_0, z_1. The latter is immediately extended to generic values of the attenuation factors, yielding

$$C_{\rm coh}(\Phi|n) = h_2\big[\tfrac{1}{2} - \tfrac{1}{2}\sqrt{1 - 4p_0p_1(1 - e^{-n|\Delta z|^2})}\big], \tag{21}$$

where $\Delta z = z_1 - z_0$ and

$$h_d[q_1, \ldots, q_{d-1}] = -\left(1 - \sum_{i=1}^{d-1} q_i\right) \log_2 \left(1 - \sum_{i=1}^{d-1} q_i\right) - \sum_{i=1}^{d-1} q_i \log_2 q_i \tag{22}$$

is the d-ary Shannon entropy. The expression in (21) is a concave function of n, hence implying that coherent states are optimal among classical transmitters in the noiseless case, i.e., $C_c(\Phi|n) = C_{\rm coh}(\Phi|n)$. For the noisy case, $n_{\rm th} > 0$, we are not able to provide an analytical expression, however, $C_{\rm coh}(\Phi|n)$ can be easily computed numerically. The numerical evaluation of $C_{\rm coh}(\Phi|n)$ suggests that it is indeed a concave function of n. This leads us to conjecture that $C_{\rm c}(\Phi|n) = C_{\rm coh}(\Phi|n)$ even in the noisy case, i.e., coherent states are optimal among classical transmitters even for $n_{\rm th} > 0$.

An approximate analytical expression for $C_{\rm coh}(\Phi|n)$ can be obtained in the limit of faint signals, $n \ll 1$, where we can approximate $|\sqrt{n}\rangle \simeq \sqrt{1-n}|0\rangle + \sqrt{n}|1\rangle$. Assuming $n_{\rm th} \ll 1$ (which is realistic in standard setups of optical reading [1]) we get to the lowest orders in $n_{\rm th}$,

$$C_{\rm coh}(\Phi|n) \simeq h_2[p_0p_1n|\Delta z|^2 + n_{\rm th}] - h_2[n_{\rm th}]. \tag{23}$$

This approximate expression for $C_{\rm coh}(\Phi|n)$ is a concave function of n, hence we conclude that, within this approximation, $C_{\rm c}(\Phi|n) = C_{\rm coh}(\Phi|n)$. Furthermore, retaining only the leading terms in $n \log_2 n$ and $n_{\rm th} \log_2 n_{\rm th}$, Eq. (23) yields

$$C_{\rm coh}(\Phi|n) \simeq n_{\rm th} \log_2 n_{\rm th} - (p_0p_1n|\Delta z|^2 + n_{\rm th}) \times \log_2 (p_0p_1n|\Delta z|^2 + n_{\rm th}). \tag{24}$$

Going beyond the set of classical transmitters we consider the state $\rho_{\rm EPR}(s,s,n) = (|\xi\rangle\langle\xi|)^{\otimes s}$ as an exemplary nonclassical transmitter. In the noiseless limit, $n_{\rm th} = 0$, an analytical expression can be easily derived for $|z_0| = |z_1| = 1$. In that case information is encoded in the relative phase $e^{i\theta}$ of the reflected modes, yielding

$$\chi[\Phi|(|\xi\rangle\langle\xi|)^{\otimes s}] = h_2\big[\tfrac{1}{2} - \tfrac{1}{2}\sqrt{1 - 4p_0p_1(1 - q_{n,s,\theta})}\big], \tag{25}$$

where

$$q_{n,s,\theta} = \left|1 + \frac{n}{s}(1 - e^{i\theta})\right|^{-2s}. \tag{26}$$

A comparison with (21) shows that a "quantum advantage" in the readout rate, i.e., $\chi[\Phi|(|\xi\rangle\langle\xi|)^{\otimes s}] - C_{\rm coh}(\Phi|n) > 0$, can be always attained (by choosing a sufficiently big s) when $\theta < \pi/2$, otherwise coherent states are always optimal probes. The situation changes if one considers generic values of z_0, z_1 [1,12] and if background thermal noise is added. Under these more general conditions one can obtain an approximate expression in the limit $n \ll 1$ by truncating the EPR state as $|\xi\rangle \simeq \sqrt{1 - n/s}|0\rangle + \sqrt{n/s}|1\rangle_{S_k}|1\rangle_{R_k}$ and $|\xi\rangle^{\otimes s} \simeq \sqrt{1-n}|0\rangle + \sqrt{n}|\aleph\rangle$ where $|\aleph\rangle = s^{-1/2}\sum_{k=1}^{s} |1\rangle_{S_k}|1\rangle_{R_k}$. If also $n_{\rm th} \ll 1$, a straightforward calculation leads to the following expression for the maximum readout rate, at the lowest orders in $n_{\rm th}$,

$$\chi[\Phi|(|\xi\rangle\langle\xi|)^{\otimes s}] \simeq h_4[p_0p_1n|\Delta z|^2, (1 - \langle|z^2|\rangle)n, n_{\rm th}] - \sum_{u=0}^{1} p_u h_3[(1 - |z_u|^2)n, n_{\rm th}], \tag{27}$$

where $\langle|z|^2\rangle = p_0|z_0|^2 + p_1|z_1|^2$. By retaining only the leading terms in $n \log_2 n$ and $n_{\rm th} \log_2 n_{\rm th}$ we finally obtain

$$\chi[\Phi|(|\xi\rangle\langle\xi|)^{\otimes s}] \simeq -p_0p_1n|\Delta z|^2 \log_2 (p_0p_1n|\Delta z|^2). \tag{28}$$

The expressions (27), (28) have several remarkable properties. First of all, they are independent of s, that is, within this approximation the number of EPR states cannot affect the reading rate, which is only a function of the overall mean photon number n. That implies $\chi[\Phi|(|\xi\rangle\langle\xi|)^{\otimes s}] \simeq \chi[\Phi||\xi\rangle\langle\xi|]$ up to higher order terms. Notice that, as suggested by the results of [1] and discussed in [12], this property does not generally hold true if $n \not\ll 1$. The second thing to be noticed is that, contrarily to (24), Eq. (28) is independent of $n_{\rm th}$, which implies that the reading rate with the EPR transmitter is insensitive to thermal-like background noise to the leading order in n and $n_{\rm th}$. In particular we have $\chi[\Phi||\xi\rangle\langle\xi|]/C_{\rm coh}[\Phi|n] \simeq \log_2 n/\log_2 n_{\rm th} > 1$ for $n < n_{\rm th} \ll 1$, that is, classical light is never optimal in this regime. On the other hand, $\chi[\Phi||\xi\rangle\langle\xi|] \simeq$

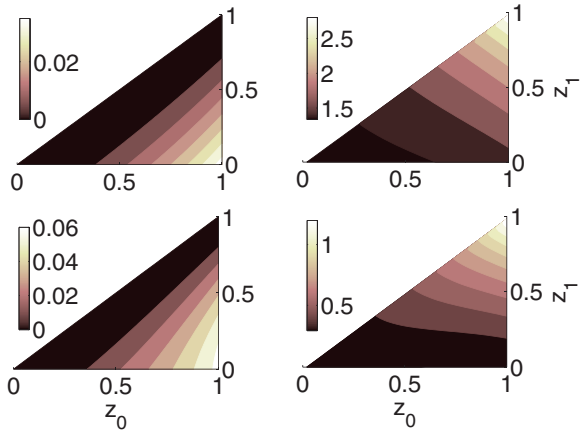

FIG. 1. (Color online) Density plots of the absolute information gain G_a (left) and of the relative information gain G_r (right) comparing the EPR transmitter with the coherent state transmitter, as a function of z_0, z_1, for positive values of the attenuating factors ($0 \leqslant z_1 \leqslant z_0 \leqslant 1$). The top plots are for $n = 0.1$, $n_{\rm th} = 1$; those on the bottom are for $n = 1$, $n_{\rm th} = 1$.

$C_{\rm coh}[\Phi|n]$ for $1 \gg n \gg n_{\rm th}$ (implying that the quantum advantage $\chi[\Phi||\xi\rangle\langle\xi|] - C_{\rm coh}[\Phi|n]$ is of higher order in this region of the parameters n and $n_{\rm th}$). Finally, it is worth remarking that both Eqs. (24) and (28) are functions of $p_0 p_1 n|\Delta z|^2$, suggesting that the approximate expressions hold true even if $n \not\ll 1$ as long as $p_0 p_1 n|\Delta z|^2 \ll 1$.

For higher values of n, $n_{\rm th}$ we resort to numerical calculations. For the sake of presentation, we put $p_0 = p_1 = 1/2$ (this choice of the probability maximizes both the noiseless coherent-state reading capacity—see Eq. (21)—and the noisy one due to symmetry reasons). Figure 1 shows numerical calculations of the absolute information gain in the reading rate,

$$G_a = \chi[\Phi|\rho_{\rm EPR}(1,1,n)] - \chi[\Phi|\rho_{\rm coh}(1,0,n)], \qquad (29)$$

and of the relative one,

$$G_r = G_a/\chi[\Phi|\rho_{\rm coh}(1,0,n)], \qquad (30)$$

provided by the EPR transmitter over the classical transmitters, for real-positive values of z_0, z_1. These plots can be compared to the analogous ones in [12] concerning the noiseless limit $n_{\rm th} = 0$. It can be noticed that, contrarily to the noiseless case, in the noisy setting the information gain is positive almost everywhere. That shows, in accordance with Eqs. (24) and (28), the robustness of quantum reading with the EPR transmitter against thermal background noise.

Figure 2 shows the information gain as a function of n and $n_{\rm th}$ for examples of amplitude encoding ($z_0 = 0$, $z_1 = 1$) and phase encoding ($z_0 = 1$, $z_1 = -1$). For amplitude encoding the gain is always positive. For phase encoding the gain is negative in the noiseless setting, that is, classical transmitters are optimal for $n_{\rm th} = 0$. However, the EPR transmitter always gives better performances for sufficiently high background thermal noise. It is worth noticing that in both amplitude and phase encoding the relative information gain allowed by the EPR transmitter is maximum for $n \ll n_{\rm th}$ in accordance with the expressions in (24) and (28).

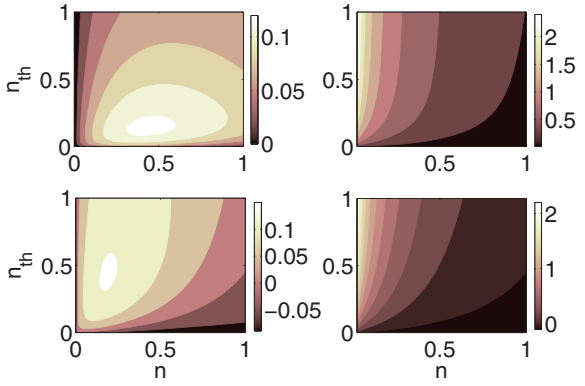

FIG. 2. (Color online) Density plot of the information gain G_a (left) and of the relative information gain G_r (right) as a function of n and $n_{\rm th}$ for amplitude encoding $z_0 = 0$, $z_1 = 1$ (top) and phase encoding $z_0 = 1$, $z_1 = -1$ (bottom).

IV. DIFFRACTION-INDUCED INTERBIT INTERFERENCE

In order to retrieve information, the probe and ancillary modes have to be collected and jointly measured. Any measurement setup must include suitable optical components to focus the incoming light on the surface of the detector. Such an optical system is characterized by its finite numerical aperture [20] which induces losses and diffraction. Because of the interference of the beams of light scattered by neighboring memory cells, the corresponding signals overlap on the detector surface [13], leading to a kind of correlated error in the reading process known as *interbit interference* [21,22]. Our aim is hence to study to what extent this kind of error limits the efficacy of the readout protocols. In order to pursue a first quantitative analysis of this kind of noise we evaluate bounds on the reading capacity in the presence of diffraction.

We model the optical system as a thin converging lens, with radius R and focal distance f. Under focusing conditions, the diffraction pattern produced by the optical system is characterized by the associated Rayleigh length, $x_{\rm R} := \lambda D_o/R$, where λ is the wavelength of a monochromatic probing light, and D_o is the distance between the memory cells and the lens. In this setting, the optical system is characterized by a set of input "normal modes," associated with the canonical operators $\{A_i, A_i^\dagger\}_{i=-\infty,\ldots,\infty}$ which are independently transmitted and attenuated by the factors $\{t_i\}_{i=-\infty,\ldots,\infty}$ (see Appendix). Thus, the optical system maps the input "normal modes" into a corresponding set of output modes $\{B_i, B_i^\dagger\}_{i=-\infty,\ldots,\infty}$ according to the relations,

$$B_i = t_i\, A_i + \sqrt{1 - |t_i|^2}\, E_i, \qquad (31)$$

where $\{E_i, E_i^\dagger\}_{i=-\infty,\ldots,\infty}$ are vacuum modes.

A monochromatic mode $\{a_j, a_j^\dagger\}$ probing the jth memory cell is scattered into a reflected mode, denoted by $\{a'_j, a'^\dagger_j\}$, with

$$a'_j = z_{u(j)}\, a_j + \sqrt{1 - |z_{u(j)}|^2}\, v_j + \nu_j. \qquad (32)$$

Moreover, we assume that the memory cells are located along a straight line of length L on the surface of the optical memory. The jth memory cell is at positions $j\ell$, where ℓ denotes the spacing between neighboring cells. In general, the scattered

modes do not form a complete set. However, they can be completed by defining a suitable set of (possibly infinite) normal modes $\{e_k, e_k^\dagger\}$ (assumed to be in the vacuum state). The input normal modes A_i's can hence be expanded as

$$A_i = \sum_j \mathcal{M}_{ij}\, a'_j + \sum_k \mathcal{N}_{ik}\, e_k, \tag{33}$$

for suitable matrices of coefficients $\mathcal{M}_{ij}$ and $\mathcal{N}_{ik}$. It follows that

$$B_i = t_i \sum_j \mathcal{M}_{ij}\, a'_j + t_i \sum_k \mathcal{N}_{ik}\, e_k + \sqrt{1-|t_i|^2}\, E_i. \tag{34}$$

In the far-field and near-field regimes it is possible to estimate the values of the attenuating factors [13]. Here we consider the near-field regime, in which $t_i \simeq 1$ for $|i| < L/x_{\mathsf{R}}$, and $t_i \simeq 0$ for $|i| > L/x_{\mathsf{R}}$ (see Appendix), yielding, for $|i| < L/x_{\mathsf{R}}$,

$$B_i = \sum_j \mathcal{M}_{ij}\, a'_j + \sum_k \mathcal{N}_{ik}\, e_k. \tag{35}$$

Since the matrix $\mathcal{M}$ has in general nonzero off-diagonal terms, the light beams reflected by different memory cells do overlap at the surface of the detector. To analyze this phenomenon, we introduce the singular value decomposition,

$$\mathcal{M}_{ij} = \sum_h \mathcal{V}^*_{hi}\, \tau_h\, \mathcal{U}_{hj} \quad (\text{for } |i| < L/x_{\mathsf{R}}), \tag{36}$$

where $\mathcal{U}$ and $\mathcal{V}$ are unitary matrices, and $\tau_h \geqslant 0$ are the (squared) singular values of $\mathcal{M}$. We can hence introduce the new sets of canonical modes $\tilde{B}_h := \sum_{|i|<L/x_{\mathsf{R}}} \mathcal{V}_{hi}\, B_i$, and $\tilde{a}'_h := \sum_j \mathcal{U}_{hj} a'_j$, in terms of which the transformation becomes diagonal,

$$\tilde{B}_h = \tau_h\, \tilde{a}'_h + \sum_{|i|<L/x_{\mathsf{R}},k} \mathcal{V}_{hi}\, \mathcal{N}_{ik} e_k. \tag{37}$$

Finally, we notice that consistency with the canonical commutation relations for the operators $\{\tilde{B}_h, \tilde{B}_h^\dagger\}$ enforces that $\sum_{|i|<L/x_{\mathsf{R}},k} \mathcal{V}_{hi}\mathcal{N}_{ik} e_k = \sqrt{1-|\tau_h|^2}\, \tilde{e}_h$, where $\{\tilde{e}_h, \tilde{e}_h^\dagger\}$ is a suitably defined set of vacuum modes. Thus, Eq. (37) expresses the fact that the modes $\tilde{a}'_h$ are independently attenuated, with attenuating factors $\{\tau_h\}$.

It is worth remarking that the independently attenuated modes $\tilde{a}'$'s do not coincide with the modes a''s carrying the information on the state of the individual memory cells. This is the very effect of diffraction, which mixes the signal scattered by different memory cells. As a consequence, the state $\rho_{\mathbf{u}^i}(s,r)$ in Eq. (2) has to be replaced with a state of the form $\rho'_{\mathbf{u}^i}(s,r) = (\mathcal{E}_{Ks} \otimes I^{\otimes Kr})\rho_{\mathbf{u}^i}(s,r)$, where $\mathcal{E}_{Ks}$ is the map describing the attenuation of the signal modes $\tilde{a}'$'s, and $I^{\otimes Kr}$ is the identity map on the remaining Kr ancillary modes. For the sake of presentation, here we assume that diffraction only involves the signal modes. The case of diffraction on both the signal and ancillary modes is simply obtained by substituting the map $(\mathcal{E}_{Ks} \otimes I^{\otimes Kr})$ with $(\mathcal{E}_{Ks} \otimes \mathcal{E}_{Kr})$. In both cases, the tensor-product structure of Eq. (2) is lost. This prevents us from expressing the reading rate in terms of a "single-letter" expression, as in Eq. (3).

Nevertheless, upper and lower bounds can be estimated by exploiting the "data processing inequality" for the Holevo information, which implies that the extra noise term expressed by the attenuating channel $\mathcal{E}_{Ks}$ can only reduce the reading rates. Such a reduction is in a range determined by the maximum and minimum values of the attenuating factors $\{\tau_h\}$, denoted by $\tau_{\max}$ and $\tau_{\min}$. We hence consider the fictitious channels $\mathcal{E}_{\max}$ and $\mathcal{E}_{\min}$ which independently attenuate all the modes $\tilde{a}'$'s by factors $\tau_{\max}$ and $\tau_{\min}$, respectively. As a matter of fact, due to the linear relation between the modes $\tilde{a}'$'s and the modes a''s, the latter are also independently attenuated by the maps $\mathcal{E}_{\max}$ and $\mathcal{E}_{\min}$. It follows that the fictitious channels do preserve the tensor product structure of Eq. (2), hence allowing us to employ the single-letter formula for the reading rate. We can hence write the following bounds for the reading rate $R[\rho(s,r)]$ in the presence of diffraction:

$$\chi[\Phi_{\min}|\rho(s,r,n)] \leqslant R[\rho(s,r,n)] \leqslant \chi[\Phi_{\max}|\rho(s,r,n)], \tag{38}$$

where $\Phi_{\min} = \{p_u, \phi_{\min,u}\}$ and $\Phi_{\max} = \{p_u, \phi_{\max,u}\}$ are the channel ensembles obtained by composition of the ensemble $\Phi = \{p_u, \phi_u\}$ with the single-mode attenuating channels with attenuating factors $\tau_{\min}$ and $\tau_{\max}$, respectively. Explicitly, the channels $\phi_{\min,u}$, $\phi_{\max,u}$, respectively, transform a probing mode $\{a, a^\dagger\}$ according to

$$a \to \tau_{\min} z_{u(j)}\, a + \sqrt{1 - |\tau_{\min} z_{u(j)}|^2}\, v + \tau_{\min} v, \tag{39}$$

and

$$a \to \tau_{\max} z_{u(j)}\, a + \sqrt{1 - |\tau_{\max} z_{u(j)}|^2}\, v + \tau_{\max} v. \tag{40}$$

A. Bounds on the reading rates

In this section, we estimate the upper and lower bounds in (38) on the reading rates in the presence of diffraction by computing the maximum and minimum of the attenuation factors τ_h's. We model the optical system associated with the measurement device as a converging thin lens of radius R, and assume that the memory cells are located along a straight line on the surface of the optical memory, where each cell has linear extension d, and neighboring cells are spaced by ℓ for a total length equal to L. A characterization of the light propagation inside such an optical system is presented in Appendix (based on [13]).

We assume that the mode describing the light reflected at the jth memory cell, on the surface of the optical memory, is of the form,

$$a'_j = \frac{1}{\sqrt{d}} \int_{j\ell-d/2}^{j\ell+d/2} dx\, A(x), \tag{41}$$

where x is a linear coordinate at the memory surface, and the continuous set of operators $\{A(x), A^\dagger(x)\}$ corresponds to the quantized amplitudes of the electromagnetic field on the surface. The latter can be in turn expressed in terms of the discrete set $\{A_h, A_h^\dagger\}$ of Fourier-transformed modes on the line [defined in Eq. (A5)]. These are the input "normal modes" which are independently attenuated by the optical system. We

hence obtain

$$a'_j = \sum_{h=-\infty}^{\infty} A_h \int_{j\ell-d/2}^{j\ell+d/2} \frac{dx}{\sqrt{dL}} \exp\left[i2\pi h\frac{x}{L} + i\theta_o(x)\right]$$
$$\simeq \sum_{h=-\infty}^{\infty} A_h e^{i\theta_o(j\ell)} \int_{j\ell-d/2}^{j\ell+d/2} \frac{dx}{\sqrt{dL}} \exp\left(i2\pi h\frac{x}{L}\right)$$
$$= \sqrt{\frac{d}{L}}\, e^{i\theta_o(j\ell)} \sum_{h=-\infty}^{\infty} \frac{\sin(\pi hd/L)}{\pi hd/L} \exp\left(i2\pi jh\frac{\ell}{L}\right) A_h, \tag{42}$$

where i stands for the imaginary unit and $\theta_o(x)$ is a position-dependent phase factor, which can be assumed to be constant on the intervals $[j\ell - d/2, j\ell + d/2]$ as long as $d^2 \ll \lambda D_o$ (see Appendix). From that we get the expression for the (adjoint of the) matrix of Eq. (33):

$$\mathcal{M}^*_{hj} = \sqrt{\frac{d}{L}}\, e^{i\theta_o(j\ell)} \frac{\sin(\pi hd/L)}{\pi hd/L} \exp\left(i2\pi jh\frac{\ell}{L}\right). \tag{43}$$

This is a rectangular semi-infinite matrix [with $j = -L/(2\ell), \ldots, L/(2\ell)$] that we will truncate by restricting it to the modes A_h's actually transmitted across the optical systems. In the near-field regime this corresponds to restrict the range to $h = -L/x_{\mathsf{R}}, \ldots, L/x_{\mathsf{R}}$, where $x_{\mathsf{R}} := \lambda D_o/R$ is the Rayleigh number (see Appendix).

The (squared) singular values of the matrix $\mathcal{M}$ are the eigenvalues of the Hermitian matrix $\mathcal{M}\mathcal{M}^\dagger$, with elements:

$$(\mathcal{M}\mathcal{M}^\dagger)_{kj} = \frac{d}{L} \sum_h \left[\frac{\sin(\pi hd/L)}{\pi hd/L}\right]^2 \exp\left[i2\pi(j-k)n\frac{\ell}{L}\right]. \tag{44}$$

In the limit $L/x_{\mathsf{R}} \gg 1$ and $\ell/L \ll 1$, we get

$$(\mathcal{M}\mathcal{M}^\dagger)_{kj} = \frac{d}{\ell} \int_{-\ell/x_{\mathsf{R}}}^{\ell/x_{\mathsf{R}}} dx \left[\frac{\sin(\pi xd/\ell)}{\pi xd/\ell}\right]^2 e^{i2\pi(j-k)x}. \tag{45}$$

The matrix $\mathcal{M}\mathcal{M}^\dagger$ is a Toeplitz matrix, with entries only depending on the difference $j-k$. The spectrum of a Toeplitz matrix is bounded by the maximum and the minimum of the Fourier transform [23],

$$f(z) = \sum_q (\mathcal{M}\mathcal{M}^\dagger)_q\, e^{-izq}, \tag{46}$$

for $z \in [0, 2\pi]$, where $(\mathcal{M}\mathcal{M}^\dagger)_q := (\mathcal{M}\mathcal{M}^\dagger)_{kj}$ for $j-k=q$. Notice that the integer q varies in the range $q \in [-L/\ell, -L/\ell]$. In the limit $L/\ell \gg 1$, the summation over q can be extended up to $\pm\infty$, yielding

$$f(z) \simeq \sum_{q=-\infty}^{\infty} \frac{d}{\ell} \int_{\frac{-\ell}{x_{\mathsf{R}}}}^{\frac{\ell}{x_{\mathsf{R}}}} dx \left[\frac{\sin(\pi xd/\ell)}{\pi xd/\ell}\right]^2 e^{i(2\pi x - z)q}$$
$$= \frac{d}{\ell} \int_{\frac{-\ell}{x_{\mathsf{R}}}}^{\frac{\ell}{x_{\mathsf{R}}}} dx \left[\frac{\sin(\pi xd/\ell)}{\pi xd/\ell}\right]^2 \sum_{m=-\infty}^{\infty} \delta\left(x + m - \frac{z}{2\pi}\right)$$
$$= \sum_{m=y/(2\pi)-\ell/x_{\mathsf{R}}}^{y/(2\pi)+\ell/x_{\mathsf{R}}} \frac{d}{\ell} \left[\frac{\sin[\pi(y/(2\pi)-m)d/\ell]}{\pi[y/(2\pi)-m]d/\ell}\right]^2. \tag{47}$$

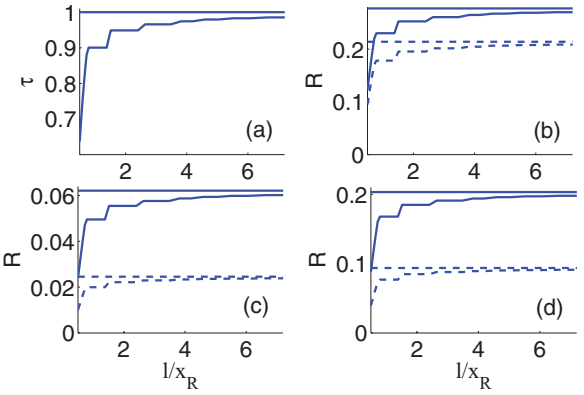

FIG. 3. (Color online) The plot shows as a function of the ratio ℓ/x_{R}: (a) the attenuating factors $\tau_{\min}$ and $\tau_{\max}$; (b), (c), (d) the lower and upper bounds on the reading rates for $p_0 = p_1 = 1/2$ with the EPR transmitter (solid lines) and the coherent-state transmitter (dashed lines). In (b) $z_0 = 0$, $z = 1$, $n = 1$, $n_{\text{th}} = 1$; in (c) $z_0 = 0$, $z_1 = 1$, $n = 0.1$, $n_{\text{th}} = 1$; in (d) $z_0 = 1$, $z_1 = -1$, $n = 0.1$, $n_{\text{th}} = 1$.

From the extrema of this function one can finally compute the attenuating factors $\tau_{\min}$, $\tau_{\max}$, and the bounds $\chi[\Phi_{\min}|\rho(s,r,n)]$, $\chi[\Phi_{\max}|\rho(s,r,n)]$.

In particular, we consider the binary marginal cell $\Phi \equiv \{p_0, p_1, z_0, z_1\}$ with $p_0 = p_1 = 1/2$ and real attenuation factors and compute the bounds on the classical reading rate by putting $\rho_{\text{coh}}(1,0) = |\sqrt{n}\rangle\langle\sqrt{n}|$ to be a single-mode coherent state of amplitude $\sqrt{n}$. As an example of a nonclassical transmitter, we also compute the bounds on the reading rate by probing with a single EPR state, $\rho_{\text{EPR}}(1,1) = |\xi\rangle\langle\xi|$. In the region with $n, n_{\text{th}} \ll 1$, these bounds can be computed according to Eqs. (23) and (27). Outside of this region, we can still compute exactly the bounds on the classical reading capacity for $n_{\text{th}} = 0$ [12]; otherwise we have to rely on numerical calculations. Figure 3 shows the bounds, for $d/\ell = 1$, as a function of the dimensionless parameter ℓ/x_{R}. The limit $\ell/x_{\mathsf{R}} \gg 1$ corresponds to the diffraction-free setting analyzed in Sec. III in which $(\mathcal{M}\mathcal{M}^\dagger)_{kj} \simeq \delta_{kj}$. On the other hand, in the region $\ell/x_{\mathsf{R}} \simeq 1$ the effects of diffraction become sensible. The choice $d/\ell = 1$ is optimal as it maximizes the value of $\tau_{\max}$, yielding $\tau_{\max} = 1$. Notice that in the high-diffraction region $\ell/x_{\mathsf{R}} < 1/2$, the lower bound $\chi[\Phi_{\min}|\rho(s,r,n)]$ becomes trivial, since $\tau_{\min} = 0$. The separation between the lower bound for the EPR state probing and the upper bound for the classical reading capacity shows that the information gain in the reading capacity persists in the presence of interbit interference caused by light diffraction.

V. CONCLUSIONS

Quantum reading exploits quantum features of light to boost the statistical discrimination of bosonic channels, which is the essential mechanism in the readout of digital optical memories. The advantages of quantum light over the classical one can be remarkable in the region of low power per pulse, a feature that may lead to technological applications for a high-density data storage device and fast memory readout. Moreover, it may allow noninvasive and reliable utilization of data storage devices based on photodegradable materials.

We have analyzed the quantum reading capacity in the presence of thermal background noise and correlated noise arising from diffraction of the probing light. We have shown that probing the memory with EPR states allows a reading rate which is, contrarily to classical states of light, mostly insensitive to thermal noise in the regime of low power per pulse. This feature mirrors the quantum advantage allowed by *quantum illumination* for the problem of target detection [24] and conveys the physical mechanism at the root of a class of two-way cryptographic protocols [26,27] (see Ref. [25] for general protocols of two-way quantum cryptography with continuous-variable systems).

Potential applications for high-density data storage technologies motivated us to study quantum reading under the effects of diffraction, which induces correlated noise in the reading process (interbit interference). By modeling the diffraction as caused by a linear optical system characterized by its Rayleigh number, we have shown that the advantage of quantum probing over the classical one persists in the presence of this kind of correlated noise.

The problem remains open of designing optimal codes and collective measurements (allowing one to achieve the optimal rates expressed by the Holevo information) which can be experimentally implemented with current technologies. This is in particular true in the presence of intersymbol interference caused by diffraction, in which case one has to face a strategy to counteract cross talks among different modes. Remarkably, an explicit capacity-achieving receiver for quantum reading has been put forward in the noiseless limit for the case in which binary information is encoded in phase, that is, $|z_u| = 1$ [28].

ACKNOWLEDGMENTS

C.L. and S.P. would like to thank S. Guha for helpful comments. The research leading to these results has received funding from the European Commission's seventh Framework Programme (FP7/2007-2013) under Grant No. 213681, the Italian Ministry of University and Research under the FIRB-IDEAS project RBID08B3FM, and Engineering and Physical Sciences Research Council under the research grant HIPERCOM (EP/J00796X/1).

APPENDIX: MODELING DIFFRACTION

Here we model the effects of diffraction by assuming that the probing light is collected and focused on the detector through a converging linear optical system. The latter is modeled as a thin lens of focal length f, which is at distances D_o, D_i from the object plane (the memory surface) and the image plane (the surface of the detector), respectively. The focusing condition is expressed by the lens law, $1/D_o + 1/D_i = 1/f$.

We assume that memory cells are disposed along a straight line on the surface of the optical memory. Let us consider the amplitude of the classical (scalar) electromagnetic field at wavelength λ, $A(x_o)$, where x_o is a Cartesian coordinate on the line at the memory surface, and the amplitude $B(x_i)$, with x_i a coordinate on the corresponding line on the detector surface. For monochromatic light, the amplitude on the object and image plane are related by the relations [20]:

$$B(x_i) = \int dx_o\, T(x_i,x_o)\, A(x_o), \tag{A1}$$

where the point-spread function is

$$T(x_i,x_o) = e^{i\theta} \int \frac{dx\, P(x)}{\lambda\sqrt{D_o D_i}} \exp\left[-i2\pi \frac{(x_i/M - x_o)x}{\lambda D_o}\right], \tag{A2}$$

$M = D_i/D_o$ is the magnification factor, and $\theta = \theta(x_i,x_o) = \theta_o(x_o) + \theta_i(x_i)$ with $\theta_o(x_o) = \pi|x_o|^2/(\lambda D_o) + 2\pi D_o/\lambda$, $\theta_i(x_i) = \pi|x_i|^2/(\lambda D_i) + 2\pi D_i/\lambda$. The function $P(x)$ is the characteristic function of the entrance pupil of the optical system. We consider a slit-shaped entrance pupil, characterized by

$$P(x) = \begin{cases} 1 & \text{for } |x| < R\,, \\ 0 & \text{for } |x| > R\,, \end{cases} \tag{A3}$$

which yields the following expression for the point-spread function:

$$T(x_i,x_o) = \frac{e^{i\theta(x_i,x_o)}R}{\lambda\sqrt{D_o D_i}} \frac{\sin[2\pi(x_i/M - x_o)/x_{\mathsf{R}}]}{\pi(x_i/M - x_o)/x_{\mathsf{R}}}, \tag{A4}$$

where $x_{\mathsf{R}} := \lambda D_o/R$ is the Rayleigh length.

For describing the propagation of light through the optical system, we consider a line element of length L at the memory surface and its image of length ML on the detector, and introduce the Fourier-transformed field amplitudes:

$$A_k := \int_{\frac{-L}{2}}^{\frac{L}{2}} \frac{dx_o}{\sqrt{L}} \exp\left[-i2\pi \frac{kx_o}{L} - i\theta_o(x_o)\right] A(x_o), \tag{A5}$$

$$B_k := \int_{\frac{-ML}{2}}^{\frac{ML}{2}} \frac{dx_i}{\sqrt{ML}} \exp\left[-i2\pi \frac{kx_i}{ML} - i\theta_i(x_i)\right] B(x_i), \tag{A6}$$

where $\theta_o(x_o), \theta_i(x_i)$ are phase factors introduced to compensate $\theta(x_i,x_o)$ in Eq. (A2). They satisfy the relation,

$$B_k = \sum_h T_{kh}\, A_h\,, \tag{A7}$$

where the *transfer matrix* has entries,

$$T_{kh} = \frac{1}{\lambda\sqrt{D_o D_i}} \int dx\, P(x) \Delta_{kh}(x), \tag{A8}$$

with

$$\Delta_{kh}(x) = \frac{1}{\sqrt{ML}} \int_{-L/2}^{L/2} dx_o \exp\left[i2\pi\left(\frac{h}{L} + \frac{x}{\lambda D_o}\right)x_o\right] \times \int_{-ML/2}^{ML/2} dx_i \exp\left[-i2\pi\left(\frac{k}{L} + \frac{x}{\lambda D_i}\right)x_i\right]. \tag{A9}$$

The expression for the transfer matrix simplifies in the near-field limit and far-field limits [13]. In particular, in the near-field limit, $L/x_{\mathsf{R}} \gg 1$ we have

$$\Delta_{kh}(x) \simeq \lambda\sqrt{D_o D_i}\, \delta_{kh}\, \delta\left(x + \frac{\lambda D_o h}{L}\right), \tag{A10}$$

yielding

$$T_{kh} = t_h\,\delta_{kh}, \tag{A11}$$

with

$$t_h = \begin{cases} 1 & \text{for} \quad |h| < L/x_{\mathrm{R}}, \\ 0 & \text{for} \quad |h| > L/x_{\mathrm{R}}. \end{cases} \tag{A12}$$

Upon quantization, the field amplitudes on the memory and the detector surface are promoted to the canonical operators $\{A_h, A_h^\dagger\}$ and $\{B_h, B_h^\dagger\}$. The form of Eq. (A11) hence implies that the modes $\{A_h, A_h^\dagger\}$ are independently attenuated with attenuation factors $\{t_h\}$, from which Eq. (31) is deduced.

[1] S. Pirandola, Phys. Rev. Lett. **106**, 090504 (2011).

[2] C. Weedbrook, S. Pirandola, R. Garcia-Patron, N. J. Cerf, T. C. Ralph, J. H. Shapiro, and S. Lloyd, Rev. Mod. Phys. **84**, 621 (2012).

[3] O. Hirota, arXiv:1108.4163.

[4] R. Nair, Phys. Rev. A **84**, 032312 (2011).

[5] M. Dall'Arno, A. Bisio, G. M. D'Ariano, M. Mikova, M. Jezek, and M. Dusek, Phys. Rev. A **85**, 012308 (2012).

[6] A. Bisio, M. Dall'Arno, and G. M. D'Ariano, Phys. Rev. A **84**, 012310 (2011).

[7] M. Dall'Arno, Ph.D thesis, University of Pavia, 2012.

[8] M. Dall'Arno, arXiv:1302.1624; M. Dall'Arno, A. Bisio, and G. M. D'Ariano, Int. J. Quantum. Inform. **10**, 1241010 (2012).

[9] M. M. Wilde, arXiv:1106.1445.

[10] A. S. Holevo, Probl. Peredachi Inf. **9**, 177 (1973).

[11] E. C. G. Sudarshan, Phys. Rev. Lett. **10**, 277 (1963); R. J. Glauber, Phys. Rev. **131**, 2766 (1963).

[12] S. Pirandola, C. Lupo, V. Giovannetti, S. Mancini, and S. L. Braunstein, New J. Phys. **13**, 113012 (2011).

[13] C. Lupo, V. Giovannetti, S. Pirandola, S. Mancini, and S. Lloyd, Phys. Rev. A **84**, 010303(R) (2011); **85**, 062314 (2012).

[14] This assumption leaves out the more general setting in which there are quantum correlations among light beams probing different memory cells [12].

[15] G. Spedalieri, C. Lupo, S. Mancini, S. L. Braunstein, and S. Pirandola, Phys. Rev. A **86**, 012315 (2012).

[16] J. Prabhu Tej, A. R. Usha Devi, and A. K. Rajagopal, Phys. Rev. A **87**, 052308 (2013).

[17] S. Guha and J. H. Shapiro, arXiv:1207.6435; S. Guha, Z. Dutton, R. Nair, J. Shapiro, and B. Yen, in *Laser Science*, OSA Technical Digest, Paper LTuF2 (Optical Society of America, Washington, DC, 2011).

[18] A. I. Lvovsky, W. Wasilewski, and K. Banaszek, J. Mod. Opt. **54**, 721 (2007).

[19] A. Ferraro, S. Olivares, and M. G. A. Paris, *Gaussian States in Quantum Information* (Bibliopolis, Naples, 2005).

[20] J. W. Goodman, *Introduction to Fourier Optics* (McGraw-Hill, New York, 1968).

[21] G. Bowen, I. Devetak, and S. Mancini, Phys. Rev. A **71**, 034310 (2005).

[22] F. Caruso, V. Giovannetti, C. Lupo, and S. Mancini, arXiv:1207.5435.

[23] R. M. Gray, *Toeplitz and Circulant Matrices: A Review* (Now Publishers, Norwell, 2006).

[24] S. Lloyd, Science **321**, 1463 (2008); S.-H. Tan, B. I. Erkmen, V. Giovannetti, S. Guha, S. Lloyd, L. Maccone, S. Pirandola, and J. H. Shapiro, Phys. Rev. Lett. **101**, 253601 (2008).

[25] S. Pirandola, S. Mancini, S. Lloyd, and S. L. Braunstein, Nat. Phys. **4**, 726 (2008).

[26] J. H. Shapiro, Phys. Rev. A **80**, 022320 (2009).

[27] Z. Zhang, M. Tengner, T. Zhong, F. N. C. Wong, and J. H. Shapiro, arXiv:1303.5343.

[28] M. M. Wilde, S. Guha, S.-H. Tan, and S. Lloyd, in *Proceedings of the 2012 IEEE International Symposium on Information Theory, ISIT 2012, Cambridge, MA, USA* (IEEE, Washington, DC, 2012), pp. 551–555.